THE ASTROPHYSICAL JOURNAL, 177:59–78, 1972 October 1

OBSERVATIONS OF THE $^2\Pi_{3/2}, J = 5/2$ STATE OF INTERSTELLAR OH

B. ZUCKERMAN
University of Maryland, College Park
J. L. YEN
University of Toronto, Toronto, Ontario
C. A. GOTTLIEB
Harvard College Observatory, Cambridge, Massachusetts 02138
AND
PATRICK PALMER*
University of Chicago
Received 1972 March 6

ABSTRACT

With the 140-foot (4267-cm) telescope of the National Radio Astronomy Observatory,[1] OH Λ-doublet radiation at 5-cm wavelength has been observed in the direction of six sources: W3, W75N, NML Cyg, W49, Sgr B2, and NGC 6334N. The $F = 3 \rightarrow 3$ transition was detected in all six sources and the $F = 2 \rightarrow 2$ transition in W3 and NGC 6334N. The lines are generally narrow and circularly polarized similar to ground-state OH maser radiation at 18-cm wavelength. The 5-cm intensities are typically a few percent of the 18-cm intensities but with wide variations from source to source. The line in NML Cyg is the first excited-state OH line detected from an infrared star; its radial velocity agrees neither with the ground-state OH nor with the H_2O velocities. An extremely peculiar time variation was observed in NGC 6334N.

I. INTRODUCTION

Λ-doublet radiation at 6-cm wavelength from the $^2\Pi_{1/2}, J = 1/2$ state of OH has been fairly well surveyed by a number of investigators (e.g., Zuckerman and Palmer 1970; Thacker, Wilson, and Barrett 1970; Palmer and Zuckerman 1970). However, the sensitivities of previous surveys at 5-cm wavelength of the $^2\Pi_{3/2}, J = 5/2$ state have not been as good as the 6-cm surveys. Five-centimeter radiation had been detected only from W3 (Yen *et al.* 1969) and from W75N (Rydbeck, Kollberg, and Elldér 1970) whereas 6-cm radiation, which is expected to be generally weaker than 5-cm radiation (Litvak, Zuckerman, and Dickinson 1969), had been observed in four sources. Accordingly we used the 140-foot telescope of the NRAO equipped with a 5-cm parametric amplifier to survey 11 ground-state OH maser sources. We have detected four new 5-cm sources; NGC 6334N was detected at about the same time by Gardner, Ribes, and Goss (1970). Preliminary results from our observations were presented at the 14th General Assembly of the I.A.U. in Brighton, England, in 1970 August (Zuckerman 1971). Below we briefly describe the equipment, then describe our spectra and discuss the results in terms of the variety of pumping models that have been proposed to explain the OH maser phenomenon.

* Alfred P. Sloan Foundation Fellow.

[1] The National Radio Astronomy Observatory is operated by Associated Universities, Inc., under contract with the National Science Foundation.

II. OBSERVATIONS

a) Equipment

The 5-cm aperture efficiency of the 140-foot telescope was 49 percent, based on an assumed peak flux density of ~57 f.u. for Virgo A. The full half-power beamwidth was 5.'1 in right ascension and 5.'2 in declination. The observations were made in the nonswitched or total-power mode where one OFF-source spectrum is subtracted from a number of ON-source spectra shifted by 0, ±2, ±4, etc., channels. This procedure sacrifices spectra near the end of the bandpass, but with the NRAO 413-channel autocorrelation receiver this is often feasible. The system temperature when looking at cold sky was ~206° K for linear polarization and ~248° K for circular polarization. (There was, in addition, 15 percent loss of signal in the circular feed.) The isolation between the two senses of circular polarization was measured to be −37 db. The temperature scales in the circular spectra (figs. 1–9) have been scaled up by 15 percent so that they agree with the linear spectra.

b) The Spectra

Figures 1–9 show the spectra. The $F = 3 \rightarrow 3$ transition was detected in six sources and the $F = 2 \rightarrow 2$ transition in two sources (negative results are given in table 1). In W3 and NGC 6334N, the sources with the most intense $3 \rightarrow 3$ radiation, an unsuccessful search was made for the $F = 3 \rightarrow 2$ and $F = 2 \rightarrow 3$ transitions. In W3 the upper limits to the $\Delta F = 1$ line intensities are ~70 times less than the intensities

TABLE 1

SUMMARY OF OBSERVATIONAL RESULTS

Source	α_{1950}	δ_{1950}	Transition	Spectral Resolution (kHz)	Radial-Velocity Range Covered (km s^{-1})	Peak-to-Peak Noise (° K)
W3(OH).....	$2^h23^m17^s$	68°38′54″	$3 \rightarrow 2$	2	−40.1, −51.3	0.4
			$3 \rightarrow 3$	2	See figures	See figures
			$2 \rightarrow 2$	2	See figures	See figures
			$2 \rightarrow 3$	2	−40.1, −51.7	0.4
VY CMa.....	$7^h20^m55^s$	−25°40′11″	$3 \rightarrow 3$	16	73.6, −29.2	0.15
			$2 \rightarrow 2$	16	68.4, −28.6	0.15
IRC 20197.....	$9^h42^m56^s$	−21°48′6″	$3 \rightarrow 3$	8	62.0, 14.5	0.4
			$2 \rightarrow 2$	8	63.3, 13.2	0.4
NGC 6334S....	$17^h16^m36^s$	−35°55′	$3 \rightarrow 3$	2	−3.1, −15.2	0.9
			$2 \rightarrow 2$	2	−3.0, −15.4	0.9
NGC 6334N....	$17^h17^m32^s$	−35°44′15″	$3 \rightarrow 2$	2	−2.4, −13.7	0.6
			$3 \rightarrow 3$	2	See figures	See figures
			$2 \rightarrow 2$	2	See figures	See figures
			$2 \rightarrow 3$	2	−2.4, −14.0	0.5
Sgr B_2(OH).....	$17^h44^m11^s$	−28°22′30″	$3 \rightarrow 3$	4	See figures	See figures
			$2 \rightarrow 2$	4	75.6, 51.7	0.5
W28N.....	$17^h58^m55^s$	−23°18′40″	$3 \rightarrow 3$	2	16.7, 5.1	0.7
			$2 \rightarrow 2$	2	17.3, 5.2	0.7
IRC 10406.....	$19^h3^m58^s$	8°9′6″	$3 \rightarrow 3$	4	61.0, 37.5	0.35
			$2 \rightarrow 2$	4	61.3, 37.5	0.35
W49.....	$19^h7^m54^s$	9°0′38″	$3 \rightarrow 3$	4	See figures	See figures
			$2 \rightarrow 2$	4	24.2, 0.2	0.3
W75N.....	$20^h36^m54^s$	42°25′40″	$3 \rightarrow 3$	2	See figures	See figures
			$2 \rightarrow 2$	2	13.6, 1.7	0.6
NML Cyg	$20^h44^m34^s$	39°56′	$3 \rightarrow 3$	8	See figures	See figures
				2	See figures	See figures
			$2 \rightarrow 2$	8	21.4, −26.5	0.35
				2	9.5, −2.2	0.7

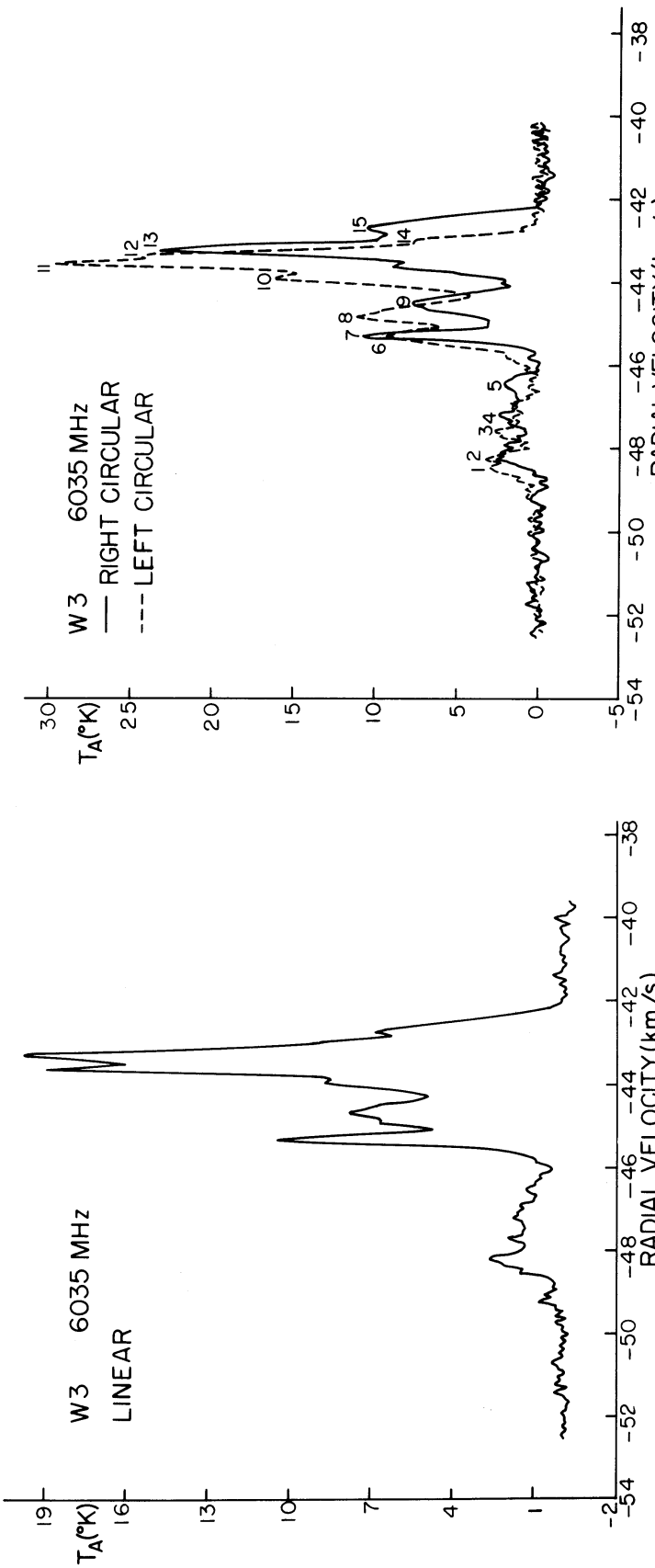

FIG. 1.—The $F = 3 \rightarrow 3$ transition in W3. *Ordinate*, antenna temperature; *abscissa*, the radial velocity with respect to the local standard of rest. The frequency resolution is 2 kHz.

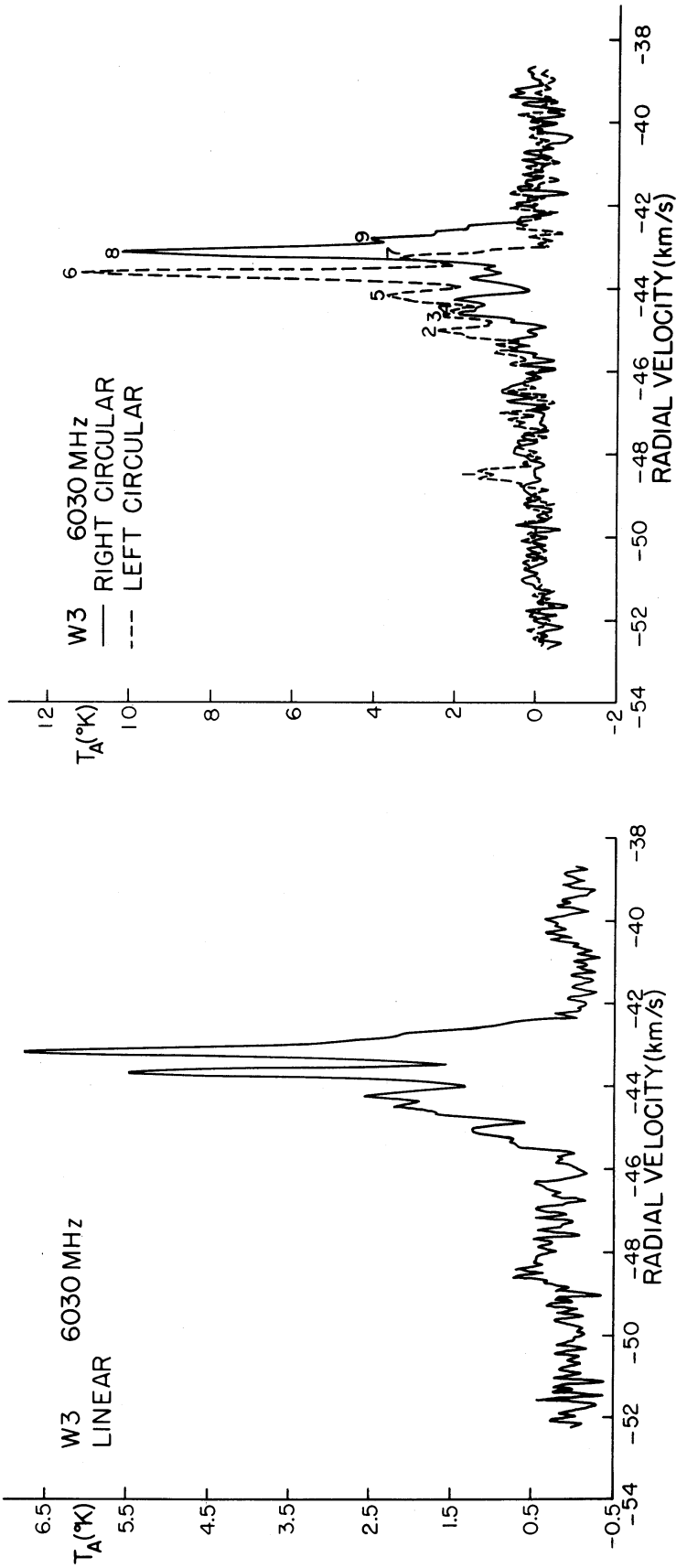

FIG. 2.—The $F = 2 \rightarrow 2$ transition in W3. The frequency resolution is 2 kHz

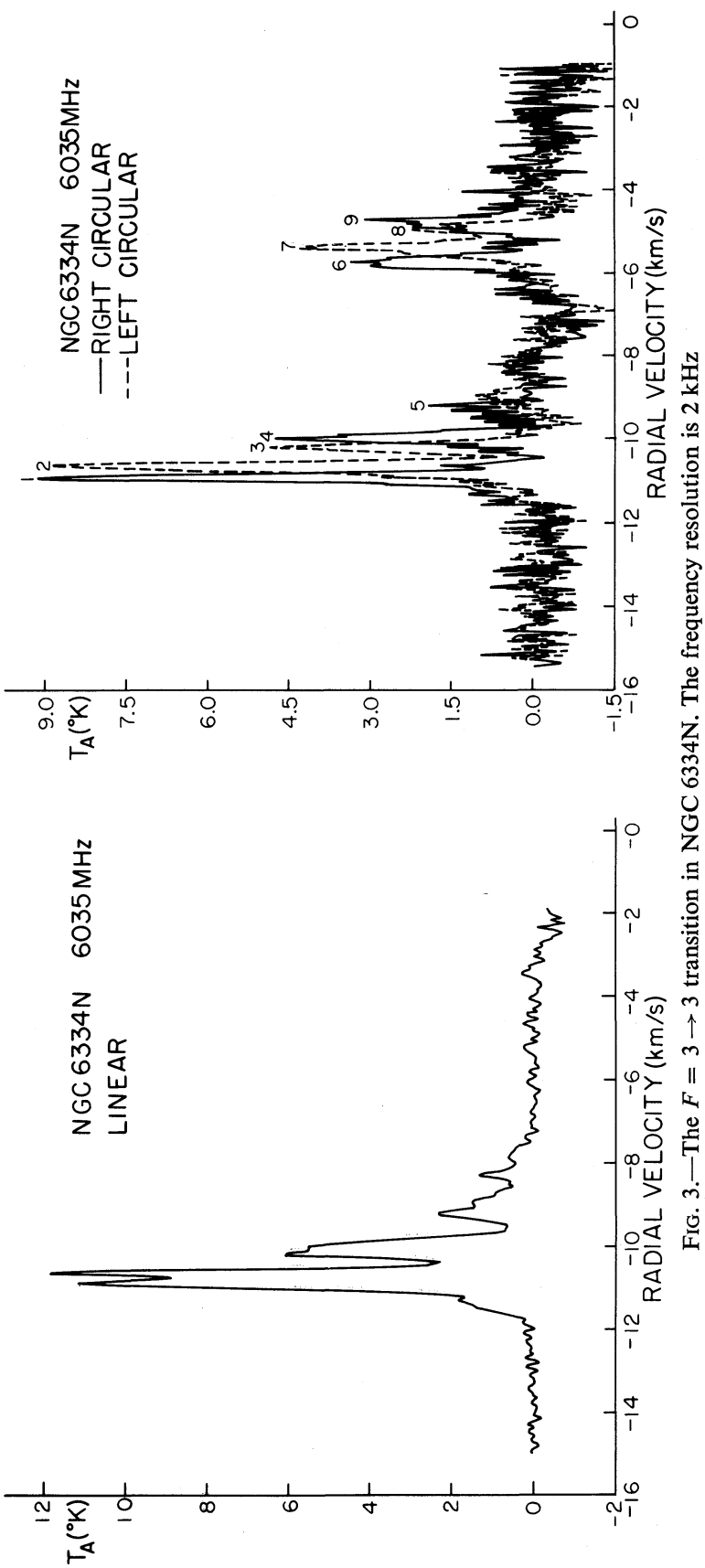

FIG. 3.—The $F = 3 \rightarrow 3$ transition in NGC 6334N. The frequency resolution is 2 kHz

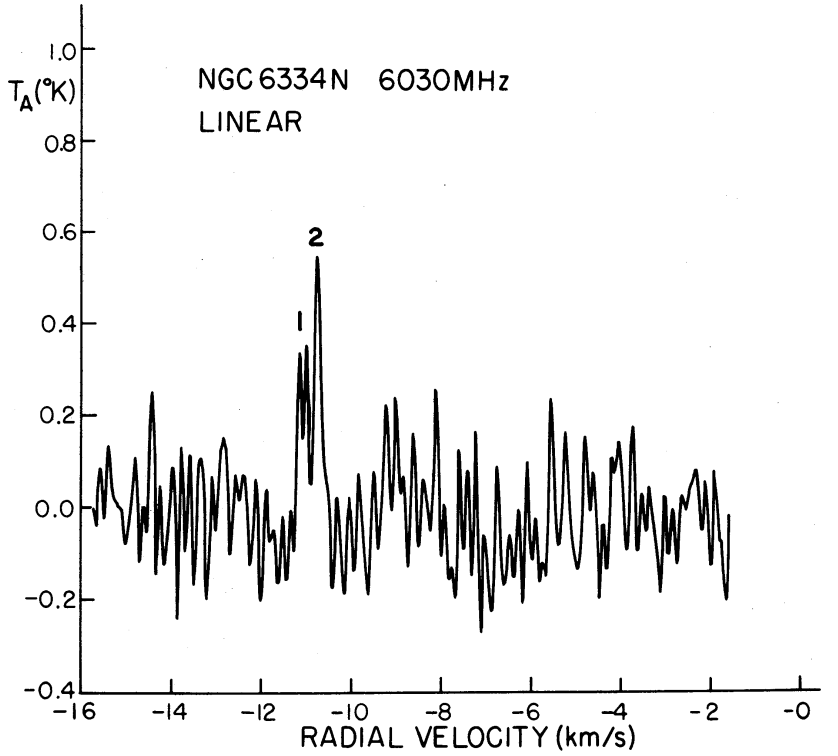

FIG. 4.—The $F = 2 \rightarrow 2$ transition in NGC 6334N. The frequency resolution is 2 kHz

of the strongest $F = 3 \rightarrow 3$ features; in NGC 6334N the corresponding number is ~ 30. Table 2 lists the percentage of circular polarization of the clearest features. The percentage of polarization is defined by $P = 100(T_{\max} - T_{\min})/(T_{\max} + T_{\min})$. Because no attempt was made to decompose the spectra into Gaussian or other simple components, the values refer to the indicated features rather than to individual components that add together to form the spectra. Percentages of circular polarization instead of Stokes parameters are tabulated because no linear polarization was detected. Column (1) gives the feature number as indicated in figures 1–9, and column (2) gives the radial velocity of the feature with respect to the local standard of rest. Column (3) lists the upper limit to the percentage of linear polarization (P_L); column (4) gives the percentage of circular polarization (P_C). The inequality signs are used in column (4) when a feature is clearly resolved in one sense of circular polarization, but occurs at a point of steep slope or at the edge of a very strong feature in the other sense of polarization. Column (5) gives the sense of polarization: R represents right-circular (a line containing only circular and unpolarized radiation is called circularly polarized) and L represents left-circular. The sense of polarization is given in parenthesis when 0 percent circular polarization is included in the error brackets.

We measured the ratio of the total amount of left-circular polarization to the total amount of right-circular polarization over the radial-velocity ranges shown in the figures. Because it was not possible to switch rapidly from left- to right-circular, some uncertainty was introduced by possible calibration variations between the measurements of the two senses of polarization. Therefore, Sgr B2 is the only source for which we can definitely state that the total energy E in left- and right-circular are unequal ($E_L/E_R = 0.47 \pm 0.3$). For all the other sources in which circular polarization was measured $E_L/E_R = 1.0 \pm 0.3$ (error bars are estimated maximum uncertainties).

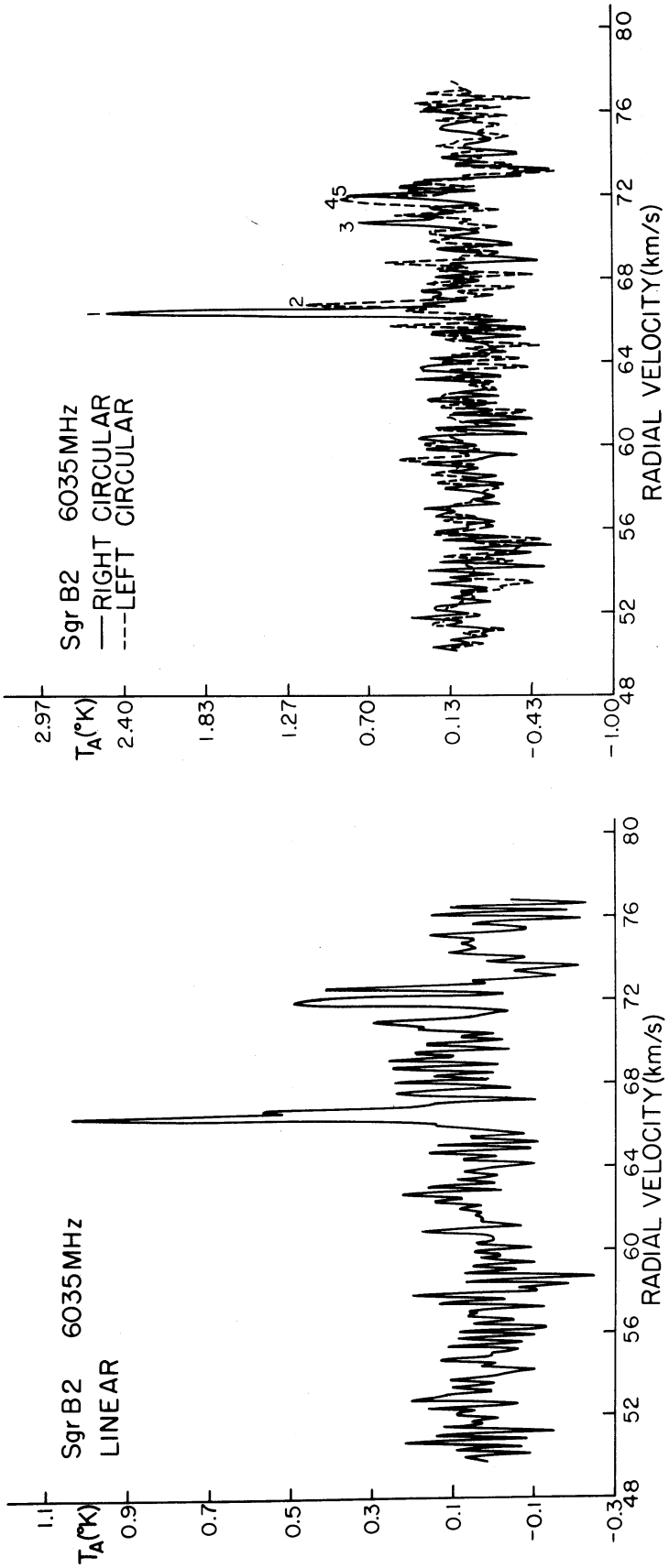

FIG. 5.—The $F = 3 \rightarrow 3$ transition in Sgr B2. The frequency resolution is 4 kHz

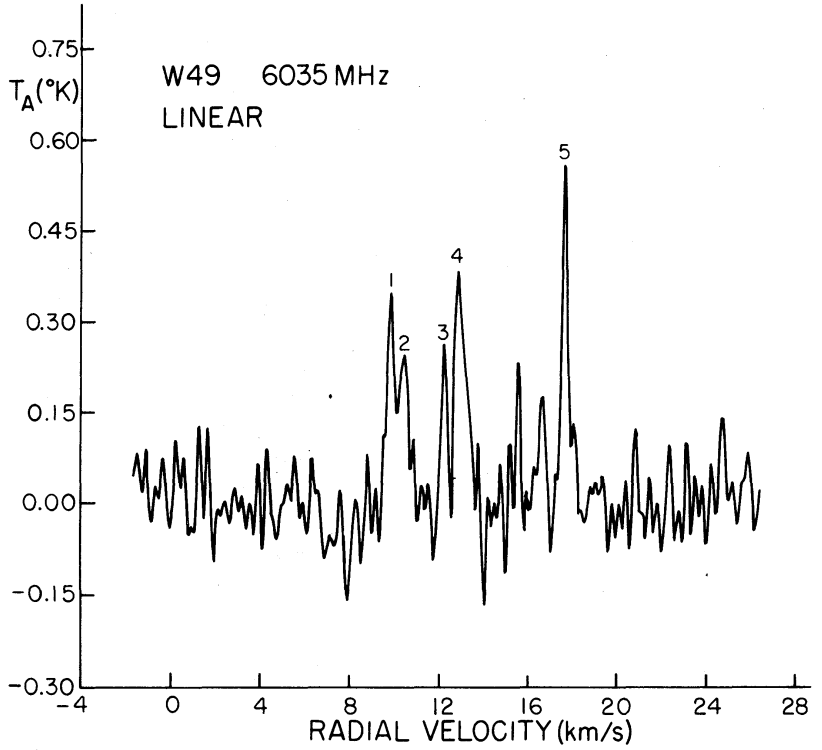

FIG. 6.—The $F = 3 \rightarrow 3$ transition in W49. The frequency resolution is 4 kHz

When comparing 5-cm spectra with ground-state spectra, one should keep in mind that the combined error in rest frequencies results in a relative uncertainty of $\sim\frac{1}{2}$ km s^{-1}.

c) *Individual Source Spectra*

i) *W3*

Figures 1 and 2 show the linear and circular spectra for the $F = 3 \rightarrow 3$ and $F = 2 \rightarrow 2$ transitions. Spectra of this source have been previously published by Yen *et al.* (1969) and Rydbeck *et al.* (1970) but with less sensitivity and/or frequency resolution. Comparison of our figures 1*b* and 2*b* with figures 4 and 5 in Rydbeck *et al.* does not indicate any obvious time variation in the spectra between 1969 August and 1970 June.

Rydbeck *et al.* have compared the portion of the spectrum between -42 and -46 km s^{-1} with other ground- and excited-state OH features in this source. However, judging from their figure 4, they were unable to detect the features between -46 and -49 km s^{-1}. The present spectrum (fig. 1) confirms the detection of $F = 3 \rightarrow 3$ radiation in this velocity range by Yen *et al.* and furthermore establishes the existence of $F = 2 \rightarrow 2$ radiation in the same general velocity range (fig. 2). The features in figures 1 and 2 around -48 km s^{-1} do not appear to have counterparts at the same velocity in any other OH transition in W3. The H_2O velocity is -46.7 km s^{-1} (Knowles *et al.* 1969).

The results in table 2 for W3 were obtained by averaging the spectra obtained with the circular feed and 2-kHz resolution (called figs. 1*b* and 2*b* below) with other circular data taken at 1-kHz resolution (but not shown). In figure 1*b* the more negative velocity side of feature 8 declines in intensity more rapidly than the more positive velocity side. In the 1-kHz spectra, where this line shape is repeated, it appears that the asymmetry

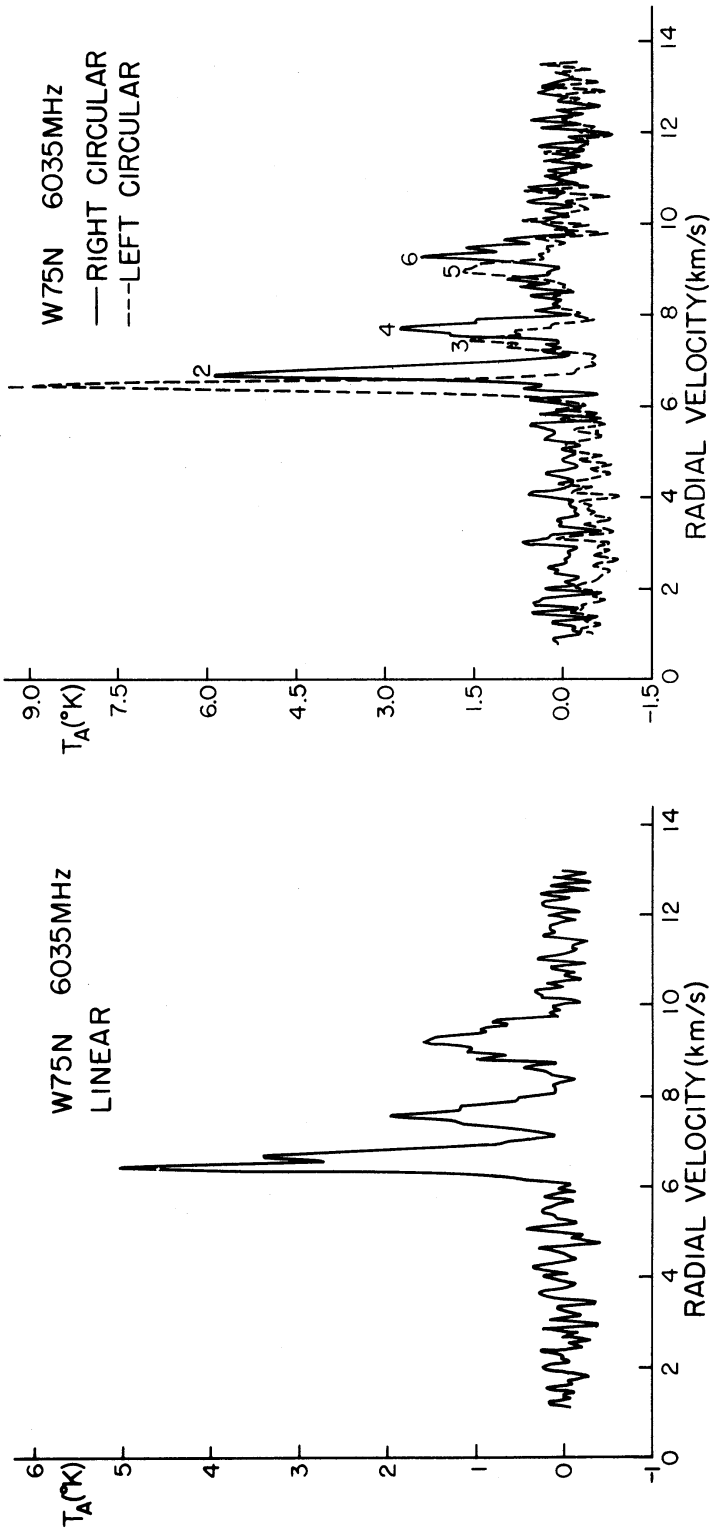

FIG. 7.—The $F = 3 \rightarrow 3$ transition in W75N. The frequency resolution is 2 kHz

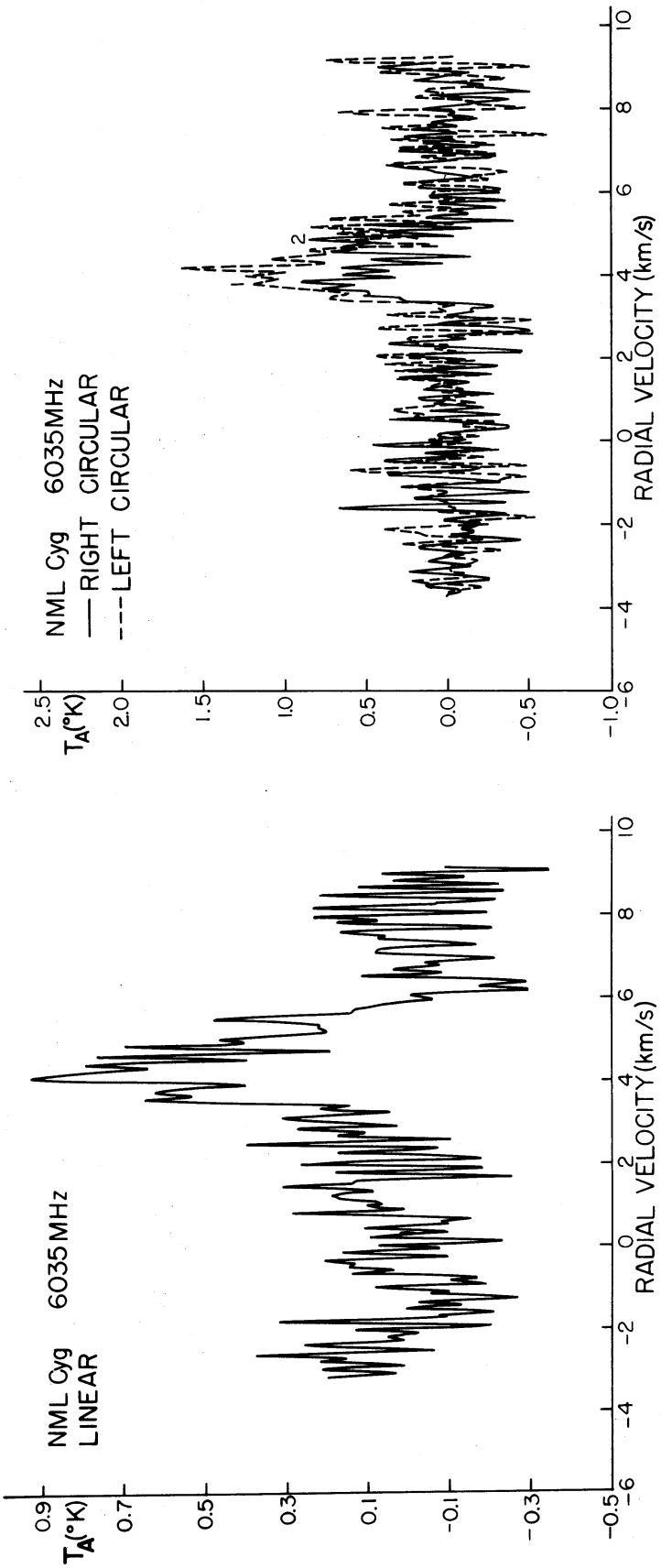

FIG. 8.—The $F = 3 \rightarrow 3$ transition in NML Cygni. The frequency resolution is 2 kHz

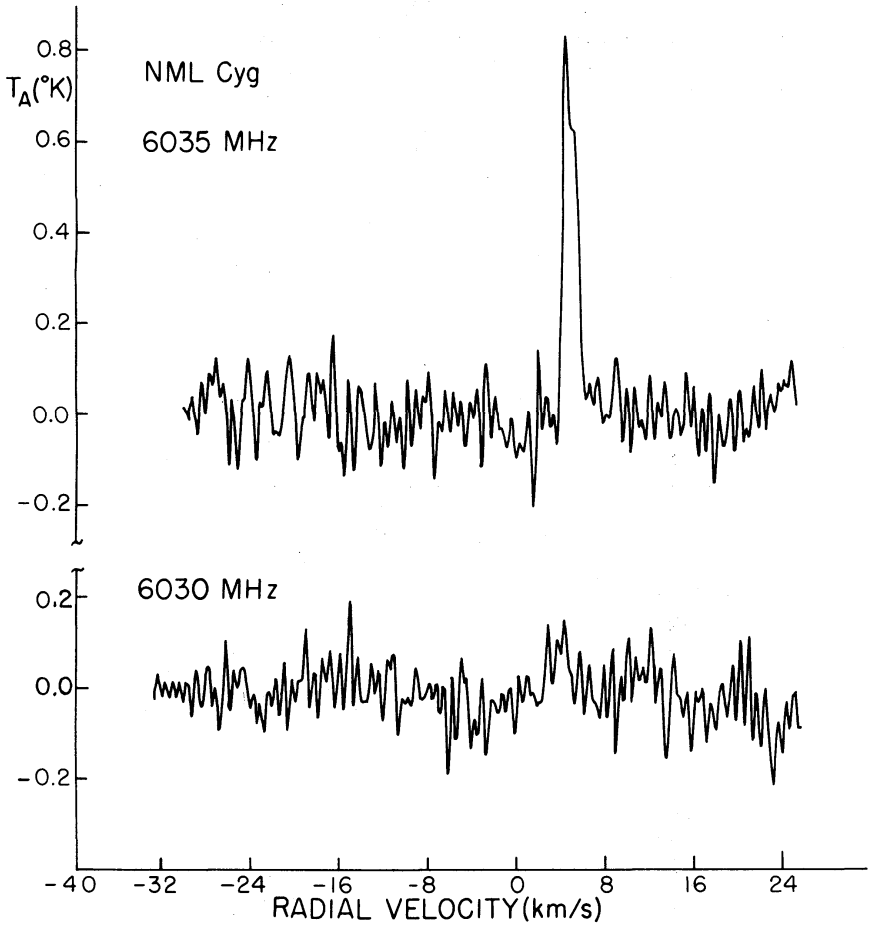

FIG. 9.—The $F = 3 \rightarrow 3$ and the $F = 2 \rightarrow 2$ transitions in NML Cygni. The frequency resolution is 8 kHz. These spectra were obtained with the linearly polarized feed.

is caused by a second Doppler feature that is blended into the (more positive velocity) side of feature 8. The higher-resolution data do not show any features beyond those indicated in figure 2*b*. However, feature 4 appears to be a single feature in the 1-kHz data, so that we have labeled it as such in figure 2*b* despite the suggestion that it may be double.

If we assume that the circularly polarized features in figures 1 and 2 are split by the Zeeman effect, we can match the strongest 5-cm features with certain of the stronger ground-state features (Barrett and Rogers 1966) as indicated in table 3. The uncertainty in rest frequencies mentioned above (± 0.25 km s^{-1} at 6030 and 6035 MHz and ± 0.40 km s^{-1} for the four 18-cm transitions) affects the velocities listed in columns (3) and (4) which, therefore, should not exactly agree among the various transitions. However, the derived B field is independent of this uncertainty. The scatter among the various fields is quite small, and even these variations may possibly be accounted for by noise in the data and inaccuracies in measuring velocities from the spectra. Despite the unequal intensities and line widths (especially in the ground state) of most of the pairs of features tabulated in table 3, the good agreement of center velocities and of derived B fields is suggestive of Zeeman patterns. Furthermore, the velocity of the second strongest feature in the $^2\Pi_{1/2}$, $J = 1/2$ state is -43.42 km s^{-1} (Zuckerman and Palmer 1970) which is, to within the errors, the same as the center of the Zeeman

TABLE 2

POLARIZATION MEASUREMENTS

FEATURE (1)	RADIAL VELOCITY (km s^{-1}) (2)	POLARIZATION (percent) Linear (P_L) (3)	POLARIZATION (percent) Circular (P_C) (4)	SENSE OF POLARIZATION (5)
		W3, 2 → 2		
1.....	−48.51	...	100 (+0, −67)	L
2.....	−45.08	...	77 (+23, −50)	L
3.....	−44.64	...	4 ± 30	(L)
4.....	−44.49	...	21 ± 24	(R)
5.....	−44.22	...	39 ± 24	L
6.....	−43.70	<16	78 ± 9	L
7.....	−43.28	...	<38 ± 11	(R)
8.....	−43.20	<14	68 ± 9	R
9.....	−42.82	...	100 (+0, −24)	R
		W3, 3 → 3		
1.....	−48.36	...	21 ± 24	(L)
2.....	−48.23	...	6 ± 20	(R)
3.....	−47.62	...	42 ± 33	L
4.....	−47.23	...	41 ± 31	R
5.....	−46.39	...	80 (+20, −41)	R
6.....	−45.35	<12	<4 ± 6	(R)
7.....	−45.29	<12	13 ± 6	R
8.....	−44.87	...	47 ± 8	L
9.....	−44.55	...	16 ± 8	R
10.....	−43.99	...	78 ± 6	L
11.....	−43.65	<9	48 ± 3	L
12.....	−43.42	<9	20 ± 3	L
13.....	−43.28	<4	>35 ± 3	R
14.....	−43.06	...	<33 ± 8	(R)
15.....	−42.72	<13	88 ± 9	R
		NGC 6334N, 2 → 2		
1.....	−11.08	...	...	...
2.....	−10.80	...	...	...
		NGC 6334N, 3 → 3		
1.....	−10.88	<26	55 ± 15	R
2.....	−10.60	<17	66 ± 17	L
3.....	−10.14	...	47 ± 27	L
4.....	−9.96	...	67 ± 33	R
5.....	−9.18	...	80 (+20, −70)	R
6.....	−5.74	...	60 ± 40	R
7.....	−5.39	...	63 ± 32	L
8.....	−4.94	...	10 ± 37	(L)
9.....	−4.78	...	42 ± 40	R
		Sagittarius B2, 3 → 3		
1.....	66.37	...	84 (+16, −32)	R
2.....	66.67	...	56 (+44, −76)	(L)
3.....	70.69	...	100 (+0, −114)	(R)
4.....	71.79	...	40 (+60, −67)	(L)
5.....	71.98	...	78 (+22, −86)	(R)

TABLE 2—*Continued*

Feature (1)	Radial Velocity (km s^{-1}) (2)	Polarization (percent) Linear (P_L) (3)	Polarization (percent) Circular (P_C) (4)	Sense of Polarization (5)
		W49, 3 → 3		
1.....	9.82	...	...	...
2.....	10.47	...	...	...
3.....	12.25	...	...	...
4.....	12.90	...	...	...
5.....	17.66	...	...	...
		W75N, 3 → 3		
1.....	6.43	...	93 (+7, −10)	L
2.....	6.66	...	78 ± 15	R
3.....	7.42	...	100 (+0, −47)	L
4.....	7.66	...	53 ± 27	R
5.....	8.95	...	89 (+11, −45)	L
6.....	9.28	...	52 ± 32	R
		NML Cygni, 3 → 3		
1.....	4.07	...	50 ± 38	L
2.....	4.81	...	27 ± 55	(R)

NOTE.—For W3 the radial velocities and the values for P_C were obtained from an average of the 1- and 2-kHz spectra (see discussion in text).

pattern in table 3. This state has a very small g-factor, and Zeeman splitting in milligauss fields would not be detectable. Thus failure to detect polarization in this state (Zuckerman and Palmer 1970) is consistent with the Zeeman interpretation. Similarly, the only feature present in the $^2\Pi_{3/2}, J = 7/2$ state has a velocity of -43.6 km s^{-1} (Turner, Palmer, and Zuckerman 1970), which agrees with the center of the Zeeman pattern to within the various uncertainties. The polarization of this line has not yet been measured. However, interferometric results (Moran *et al.* 1968) at 1665 MHz show that the -45.5 and -41.7 km s^{-1} features are spatially separated, suggesting that the possible Zeeman patterns are simply due to chance coincidences. Further interferometric results at 5 and 18 cm may settle this question. At the very least, at both 5 and 18 cm the left-circular features appear to be systematically at more negative radial velocities than the right-circular features. Rydbeck *et al.* (1970) have also attempted to fit Zeeman patterns in W3, but their signal-to-noise ratio was not as good as in the present experiment.

ii) *NGC 6334N*

Figures 3 and 4 show the linear and circular spectra for the $F = 3 \rightarrow 3$ and $F = 2 \rightarrow 2$ transitions. Comparison of these spectra with the ground-state spectra of Ball and Meeks (1968), Weaver, Dieter, and Williams (1968), and Robinson, Goss, and Manchester (1970) shows both 18- and 5-cm features over the radial-velocity range -7.5 to -12 km s^{-1} although there is little, if any, detailed correspondence of features. There is a possible anticorrelation of 1665-MHz with 6035-MHz features in the -10 to -11 km s^{-1} range, whereas, in contrast, both 1667 and 1720 MHz are

TABLE 3

POSSIBLE ZEEMAN PATTERNS

Source (1)	Transition (MHz) (2)	Feature Velocity (km s^{-1}) (3)	Center Velocity (4)	B (milligauss) (5)
W3	6030	−43.7(L) −43.2(R)	−43.45	6.35
	6035	−43.65(L) −43.27(R)	−43.46	6.75
	1665	−45.5(L) −41.7(R)	−43.60	6.45
	1667	−44.75(L) −42.33(R)	−43.54	6.85
	1720	−44.1(L) −43.4(R)	−43.75*	6.2†
NGC 6334N	6030	−11.08‡ −10.8	−10.94	3.6
	6035	−10.88(R) −10.60(L)	−10.74	5.0
	1665	−12.36(R)§ −8.94(L)	−10.65	5.8
	1665	−12.18(R)§ −8.94(L)	−10.56	5.5
	1667	−12.00(R) −10.02(L)	−11.01	5.6
	1720	−11.09(R) −10.19(L)	−10.64*	8.0†

* Based on line rest frequency of 1720.528 MHz.

† Based on identifying the observed features with the strongest components of the Zeeman pattern (Palmer and Zuckerman 1967).

‡ Based on linear spectrum—fig. 4.

§ Two possible velocities for right circular feature (see Robinson *et al.* 1970).

Note added on 1972 April 15.—The radial velocities in the table are based on rest frequencies of 1612.231, 1665.401, 1667.358, and 1720.528 MHz. With the newer, more accurate rest frequencies of ter Meulen and Dymanus (1972), the radial velocities for the 1665-, 1667-, and 1720-MHz features should be slightly revised. This revision improves the agreement of center velocities of the 5- and 18-cm Zeeman patterns in W3. In NGC 6334N the agreement (with the 5-cm pattern) is improved for the 1667-MHz transition but made substantially worse for the 1665- and 1720-MHz transitions. Throughout the paper, the 5-cm OH rest frequencies are those measured by Radford (see Yen *et al.* 1969).

strong in this velocity range. This is to be expected if we are observing Zeeman patterns (see below).

The most interesting features in NGC 6334N are present in figure 3*b* between −4.5 and −6 km s^{-1} but are entirely absent in figure 3*a*. No ground-state features have been observed at this velocity. H_2O has been observed at a velocity of −3 km s^{-1} (Meeks *et al.* 1969). Our observations of these features (summarized in table 4) suggest time variations, $\Delta T_{\text{antenna}}/T_{\text{antenna}} \sim 1$, on a scale of < 12 hours. The variations may have been much faster than this if the decrease between June 4 and 5 was non-uniform or if the actual intensity on June 2 or 5 was well below our detection limit. These time variations are an order of magnitude faster than any reported for ground- and excited-state OH and for H_2O.

One might wonder if the rapid variation is due to instrumental problems or other causes. We feel this is unlikely for the following reasons.

1. We find good agreement among the shapes of the features between −10 and

TABLE 4

TIME VARIATIONS IN NGC 6334N

Day (1970)	Local Sidereal Time	Polarization	T_A (° K)
June 2.....	16^h16^m–18^h19^m	Linear	<0.3
June 4.....	16^h40^m–19^h12^m	Circular	4.0*
June 5.....	17^h30^m–18^h36^m	Linear	<0.3

* Scaled to gain of linear feed.

-11 km s^{-1} when comparing the average of the data of June 2 and 5 with the average of the left- and right-circular spectra.

2. The telescope pointing was accomplished by peaking up on the NGC 6334 continuum position and offsetting to the 18-cm OH position. The telescope position on June 2, 4, and 5 was recorded in the observer's log and by the computer. Because the antenna temperature in the features at -10 and -11 km s^{-1} in the circular spectra is somewhat weaker than would be expected from the linear spectra (after correction by the above-mentioned 15 percent scaling factor), it is possible that the antenna was not pointed at quite the same position on June 4 as it was on June 2 and 5. Then because of a "pointing error" on June 4 one might pick up some features that were just outside of the beam on June 2 and 5. We regard this possibility as highly unlikely for the following reasons. The size of the required "pointing error" ($\sim 2'$ for the most favorable geometry and assuming that the true peak antenna temperature in the variable features is < 10 times greater than the observed value) seems unreasonably large considering the computer pointing record and the method of pointing. Furthermore, the operator would have had to make essentially the same pointing error while setting the telescope for the left-circular and the right-circular observations, which were separated by ~ 100 minutes. Finally, the region around NGC 6334 has been extensively studied at 18 cm with both single antennas and interferometers and there is no indication of an OH source closer to NGC 6334N than NGC 6334S. If the variable 5-cm features are actually coming from a position displaced from NGC 6334N, then they represent the first source with excited-state but no ground-state OH emission. A 5-cm map of the region around NGC 6334N in 1971 June yielded a negative result at the velocities of the variable features. Then the only alternative to accepting the rapid (12-hour) variation as real is to interpret our results as a combination of a displaced source and slow time variations. However, from the above discussion, we regard the latter possibility as highly unlikely. (The 1971 June results will be discussed in a forthcoming paper.)

3. There were no problems with interference during our observing run. Furthermore, the variable features are circularly polarized and look just like "typical" 5-cm OH lines.

4. We rotated the feed on June 5. Therefore, it is not possible that the variable features are highly linearly polarized and that we happened to be looking at the position angle of minimum intensity on June 2 and 5.

5. NGC 6334N was observed at 5 cm on 1970 June 16–17 with the 210-foot (64-m) Parkes antenna (Gardner *et al.* 1970). The agreement with our spectra in the non-variable range (considering the differences in velocity resolution) is good. The variable features are not present in the Australian spectra.

We also investigated the variable features for minute-by-minute variations. None were observed outside of the expected noise fluctuations.

We have attempted to fit Zeeman patterns to our 5-cm observations and those of

Robinson *et al.* (1970) at 18 cm. From table 3 one can see that the fit is not quite as good as for W3. However, because the 18-cm spectra in NGC 6334N are simpler than in W3, the chance of obtaining even such a fit by accident would seem to be quite small. A weak 6-cm OH feature has been observed at -10.3 km s^{-1} from the $^2\Pi_{1/2}$, $J = 1/2$ state (Thacker *et al.* 1970). This velocity does not quite agree with the central velocity of the Zeeman pattern. The magnetic fields suggested by the other pairs of features in table 2 (those not listed in table 3) range between 3 and 6 milligauss.

iii) *Sagittarius B2*

Figure 5 shows the linear and circular spectra for the $F = 3 \rightarrow 3$ transition. Although the 5-cm radiation between 66 and 73 km s^{-1} falls in the general velocity range of strong ground-state emission, there may nevertheless be an anticorrelation between the 5- and 18-cm features. In particular, 1665-, 1667-, and 1612-MHz features are all strongest at a velocity of 67 to 69 km s^{-1} (Palmer and Zuckerman 1967) where there is little if any 6035-MHz radiation. The displacements between the 5-cm and the strongest 18-cm features are typically a few kilometers per second. Then one might try to explain the apparent anticorrelation as due to different Zeeman shifts among various lines originating in the same cloud. The fields deduced from the 5-cm lines are 4 milligauss. Left-circular features at 68.1 (1665 MHz) and 67.5 (1667 MHz) km s^{-1} are consistent with the 5-cm splittings (of the 66.67 and 66.37 km s^{-1} features), but the corresponding right-circular features are not present and no 18-cm features match the 5-cm lines at 71.79 and 71.98 km s^{-1}. No OH in other excited rotational states has been observed between 66 and 73 km s^{-1}. The H_2O velocity in Sgr B2 is 71.4 km s^{-1} (Meeks *et al.* 1969).

Ground-state spectra obtained ~ 3 years after those of Palmer and Zuckerman (1967) show no obvious time variations in the velocity range 66–73 km s^{-1} (Robinson *et al.* 1970). However, at other velocities in the ground-state spectrum there are two examples of apparent time variations. At 1667 MHz Palmer and Zuckerman observed two right-circular features (called 4 and 5 in their paper) at velocities of ~ 55 and 56 km s^{-1}, whereas Robinson *et al.* observed right-circular features at velocities of ~ 54.5 and 55 km s^{-1}. Although there was no obvious variation in the 55 km s^{-1} feature, the 56 km s^{-1} feature appears to have been "replaced" by the feature at 54.5 km s^{-1}. At 1720 MHz there is a left-circular feature at 60 km s^{-1} in Robinson *et al.* that is not present in the spectra of Palmer and Zuckerman. (Note that in these two papers the 1720-MHz rest frequencies that were used differed by 1 km s^{-1}.)

iv) *W49*

Figure 6 shows the linear spectrum of the $F = 3 \rightarrow 3$ transition. Because of the weakness of these features there was insufficient time to obtain circular spectra. There appears to be a general anticorrelation of the velocities of 5-cm features with velocities of ground-state features in all four 18-cm transitions (Palmer and Zuckerman 1967). The only feature in the $^2\Pi_{1/2}$, $J = 1/2$ state in this source is at a velocity of 8.2 km s^{-1} (Zuckerman and Palmer 1970).

There is a suggestion of "Zeeman" doublets in the features in figure 6, although circularly polarized spectra are required to confirm this possibility. If the splittings of ~ 0.65 km s^{-1} (see table 2) are magnetic, the implied field strength is ~ 12 milligauss. The predicted ground-state features at 1665 and 1667 MHz are not present in either sense of polarization.

v) *W75N*

Figure 7 shows the linear and circular spectra for the $F = 3 \rightarrow 3$ transition. Comparison with data of Rydbeck *et al.* (1970) suggests that in 1970 between January and

June the only "obvious" time variation occurred in the left-circular feature at 6.43 km s^{-1}. Comparison of their figure 1 with our results suggests that the ratio of the intensities in the left (6.43 km s^{-1}) to right (6.66 km s^{-1}) features increased by a factor of ~ 1.5 during this time interval. The reality of this variation does not depend on the somewhat uncertain gains in the two senses of circular polarization (see above) since the variation is evident from the linear spectra alone. The intensity ratio in the two features in question in 1970 June is intermediate between the 1969 August and 1970 January ratios. Variations in the ground state appear to be small (cf. Zuckerman *et al.* 1969; Rydbeck *et al.* 1969, 1970) except at 1667 MHz where the left-circular feature at 5.5 km s^{-1} monotonically increased in amplitude by a factor of ~ 10 between 1968 July and 1970 January. We see no evidence for a cyclic (5-month) variation as suggested by Rydbeck *et al.* (1970).

Once again there is an anticorrelation in velocities between the ground- and excited-state features. The only "good" coincidence is at 9.3 km s^{-1} where there are weak right-circular features at both 5 and 18 cm. Rydbeck *et al.* (1970) attempted to fit consistent Zeeman patterns between the 5- and 18-cm lines (which would account in part for the anticorrelation in velocity). With the three pairs of 5-cm lines (splittings corresponding to ~ 5 milligauss) one can predict the positions of the corresponding Zeeman-split lines at 1665 and 1667 MHz. There are a couple of coincidences (which, however, can probably be attributed to chance), but on the whole there is little agreement between 5- and 18-cm patterns.

vi) *NML Cygni*

Figures 8 and 9 show the linear and circular spectra for the $F = 3 \rightarrow 3$ and $F = 2 \rightarrow 2$ transitions. The $F = 3 \rightarrow 3$ feature is the first and, as yet, only excited-state OH line observed in an infrared star. The 5-cm velocities agree with neither the 18-cm OH (Wilson, Barrett, and Moran 1970) nor the H_2O velocity of -19 km s^{-1} (Schwartz and Barrett 1970). The splitting between the left- and right-circular 5-cm features corresponds to a field of 13 milligauss. There is a possible $F = 2 \rightarrow 2$ feature in figure 9 at a velocity of ~ 4 km s^{-1}. Normally we would not consider this to be a significant peak except that it agrees reasonably well with the velocity of the $F = 3 \rightarrow 3$ feature. Further observations are needed to establish the reality of the $2 \rightarrow 2$ feature.

III. DISCUSSION

The geometry of the OH masers is still uncertain, and a number of models have been suggested to explain the observations. The interferometer picture (in W3) is of numerous spots, ~ 30 a.u. in size, contained in a region $\sim 10^4$ a.u. in diameter (Moran *et al.* 1968). In one class of models the maser amplification takes place only in the spots themselves; in another class of models amplification is along the entire path of 10^4 a.u. In either case one envisions hydrogen atom plus molecule densities $n_H + n_{H_2} \lesssim 10^7$ cm^{-3} so that collisions across the Λ-doublets and collisional de-excitation of rotation do not significantly lessen the population inversion. Alternative models relying on collisional or chemical pumping entirely within the spots suggest densities between 10^{10} and 10^{13} cm^{-3} (e.g., Rank, Townes, and Welch 1971). Certain problems with this class of models have been discussed by Litvak (1969)—in particular, the elimination of population inversion and hyperfine anomalies due to collisional quenching of the rotational far-infrared fluorescence. Another problem is the small surface area of the spot which does not allow adequate gain or loss of the ~ 100-μ OH resonance photons that accompany all pumping processes. Comparison of the present OH spectra with those at 6, 18, and 2.2 cm indicates that the strength of the maser output decreases as one goes up the rotational energy ladder. If $n_{H_2} > 10^{10}$ cm^{-3}, then this decline in

intensity is likely only if $T < 40°$ K, so that even the $\Pi_{3/2}$, $J = 5/2$ state at 84 cm^{-1} is significantly less populated than the ground state (this assumes that the fractional inversion in the ground state is not substantially larger than in the excited states). At this low temperature it is difficult to account for the observed intensity of the $\Pi_{3/2}$, $J = 7/2$ line in W3 (Turner *et al.* 1970) unless it originates in a hotter region than the 18-cm emission. Interferometric observations may be useful here.

Furthermore, if $n_{H_2} \gtrsim 10^{10}$ cm^{-3}, it is difficult to explain the variety of hyperfine anomalies that have been observed at 5, 6, and 18 cm. When $n_{H_2} > 10^7$ cm^{-3}, the collision rate across the Λ-doublets, $K_c n_{H_2}(s^{-1})$, is larger than the spontaneous far-infrared de-excitation rate, $A_{IR}(s^{-1})$. Then the optical depth in the Λ-doublet maser transition is proportional to $\Delta n_{OH} l = \eta n_{OH} l[1 + (K_c n_{H_2}/A_{IR})]^{-1}$, where η is the intrinsic pump efficiency and l is the total path length over which amplification occurs. Here we have neglected the effects of infrared trapping which effectively reduces A_{IR} and thus decreases the optical depths; see equation (7) in Litvak *et al.* (1969), where $K_c n_{H_2} = C$. Also neglected in the expression for $\Delta n_{OH} l$ is a term that represents ordinary thermalizing collisions which are always present between the Λ-doublet levels. [This term is written as $-(n_u + n_l)\Delta C$ in eq. (2) in Litvak *et al.* 1969.] If this effect, which is proportional to density, is not to completely destroy the inversion at high densities, then the pump rate per molecule must also increase proportionally with the density. This seems possible only for collisional or chemical pumps since no reasonable radiational pump has been suggested that can compete with collisions at densities greater than 10^{10} cm^{-3}. At low densities ($A_{IR} \geq K_c n_{H_2}$), we can obtain just enough unsaturated amplification within the spots ($l \sim 5 \times 10^{14}$ cm) to account for the observed intensities, assuming that $\eta = 1$ percent and that 1 percent of the O is in the form of OH. At high densities n_{OH} must increase as n_{H_2} to keep $\Delta n_{OH} l$ constant (i.e., a large projected density of OH compensates for the low pump efficiency. We have optimistically assumed that $\eta = 1$ percent even at high densities). Then, however, $\tau_{far\,IR} \gg 1$ for all allowed rotational transitions, and differential escape of these photons from the OH cloud, which might lead to some hyperfine anomalies, will not occur. Then it is not clear how internal volume pumps such as the nonequilibrium collisions between H and OH suggested by Gwinn and Townes (see Litvak *et al.* 1969), or perhaps a competition between OH and hotter (or cooler) dust for the far-infrared photons, can explain the variety of observed hyperfine patterns since these processes are not sensitive to the hyperfine splittings. Also, specific hyperfine patterns are usually associated with specific astrophysical environments (e.g., H II regions and 1665 MHz or infrared stars and 1612 MHz). Because of the very large OH and dust optical depths in the near- and far-infrared and the ultraviolet there is no hope of getting outside information into one of these dense blobs. Even at 100 μ, $\tau_{dust} > 1$ for $n_H l > 10^{24}$ cm^{-2}; see Litvak *et al.* (1969). Then it is far from obvious why there should be an association of hyperfine patterns and specific astrophysical objects under these high-density conditions. Finally, in the absence of radiational pumps that transmit information at the velocity of light, it is extremely difficult to understand what could produce an intensity variation by a factor of 10 in NGC 6334N on a timescale of $\lesssim 12$ hours.

These considerations indicate low-density objects, such that $A_{IR} > K_c n_{H_2}$. If amplification is occurring entirely within the interferometer spots, then these might be regarded as density fluctuations in a more extended, somewhat lower density medium (the spots themselves are far from gravitationally bound, although the whole 10^4 a.u. region could be bound). The rapid (12-hour) time variation observed in NGC 6334N suggests a maximum size to the region in which the variable features are amplified. If these features are well saturated, then the implied source size is $\lesssim 80$ a.u. If these features are unsaturated, then an intensity variation by a factor of ~ 10 could be produced in a region of dimensions $\lesssim 10^3$ a.u. within a space of 12 hours. Typical intensity variations in the ground state are much slower, of order weeks or longer (e.g.,

Zuckerman *et al.* 1969). This characteristic time is consistent with amplification over path lengths of 10^4 a.u. (for which the light travel time is ~ 1 month), as suggested in some models. However, for this amplification length it is not clear how to produce the rapid variation observed in NGC 6334N unless the amplifier is unsaturated, is very long and skinny (a filament), and is oriented so that the velocity dispersion along the path is $\lesssim 1$ km s^{-1}. An alternative model has been suggested by Litvak (1971) where the maser is a roughly spherical cloud with a small (~ 30 a.u.) unsaturated core surrounded by a larger (10^4 a.u.) region of saturated amplification. However, if the maser is well saturated, then the output intensity, integrated over the area of a spot, is rather insensitive (on timescales of $\lesssim 12$ hours) to even large changes in pumping conditions in the core. If the integrated intensity was only slightly larger than the intensity after amplification in the unsaturated core, perhaps the rapid changes could be accounted for—then, however, this model becomes essentially the same as those models where amplification occurs only in the spots. Therefore, for the rapidly variable features in NGC 6334N, amplification in $\lesssim 10^3$ a.u. seems most plausible. Nevertheless, because this phenomenon has been observed only once and interferometric observations were not obtained, one cannot rule out models in which amplification for the vast majority of Doppler features occurs over 10^4 a.u.

Collisional-pumping models such as that of Gwinn and Townes suggest that excited- and ground-state inversion and, hence, emission should be present at the same Doppler velocity. The present results indicate that this is not the case and that, if anything, there appears to be an anticorrelation between the 5- and 18-cm velocities. Possibly some of this anticorrelation is the result of different Zeeman shifts. However, if the 5-cm features have been properly paired into Zeeman doublets, then this effect will not satisfactorily explain the anticorrelation in most sources (see above discussion of individual sources). An interesting question is: Are we observing the Zeeman effect? In W3 and NGC 6334N (see table 3) there appears to be a reasonable approximation to a Zeeman pattern. Yet the interferometric observations in W3, which show the -45.5 and -41.7 km s^{-1} features to be spatially separated, apparently argue against this interpretation. (It appears unlikely that the separation can be attributed to differential refraction of the left- and right-circular rays between the source and the radio telescope.) If the Zeeman effect is not important and if the spots are essentially independent maser clumps, it is not yet clear why in the above two sources and in W75N there appears to be a fairly systematic arrangement of left-circular features at either more positive or more negative velocities than the right-circular features. Litvak (1971) has suggested that this type of effect could be due to a rotational discontinuity between two parallel corotating disks. At the risk of being obvious, interferometric observations are sorely needed at 2.2, 5, and 18 cm. Possibly the anticorrelation in velocity indicates that the 5-cm lines originate in hotter, more dense regions than the 18-cm lines.

IV. SUMMARY

$\Delta F = 0$ OH radiation has been observed at 5-cm wavelength from six galactic sources. Because of the time variations in two sources and the peculiar intensity ratios among the four hyperfine lines, we interpret this as maser radiation, although source sizes have not yet been measured. Arguments have been given against high-density models for which collisional rates are faster than spontaneous far-infrared rates. The strongest excited-state lines are observed from OH sources near H II regions; infrared stars are weaker emitters of 5- and 6-cm radiation. Possible Zeeman patterns were observed in a number of sources. However, interferometric observations at 5, 18, and 2.2 cm are required to settle this and other problems.

We thank Mr. Craig Moore for his help with the equipment, and J. A. Ball for assistance. B. Z. thanks Dr. Peter Goldreich and Dr. Marvin Litvak for useful discussions and the California Institute of Technology for their hospitality during a visit where part of this work was carried out. Partial financial support for this work came from NSF grants GP-14302 to the University of Maryland, GP-25225 to the California Institute of Technology, GP-19717 to Harvard University, and GP-13464 to the University of Chicago.

REFERENCES

Ball, J. A., and Meeks, M. L. 1968, *Ap. J.*, **153**, 577.
Barrett, A. H., and Rogers, A. E. E. 1966, *Nature*, **210**, 188.
Gardner, F. F., Ribes, J. C., and Goss, W. M. 1970, *Ap. Letters*, **7**, 51.
Knowles, S. H., Mayer, C. H., Cheung, A. C., Rank, D. M., and Townes, C. H. 1969, *Science*, **163**, 1055.
Litvak, M. M. 1969, *Science*, **165**, 855.
———. 1971, *Ap. J.*, **170**, 71.
Litvak, M. M., Zuckerman, B., and Dickinson, D. F. 1969, *Ap. J.*, **156**, 875.
Meeks, M. L., Carter, J. C., Barrett, A. H., Schwartz, P. R., Waters, J. W., and Brown, W. E., III. 1969, *Science*, **165**, 180.
Moran, J. M., Burke, B. F., Barrett, A. H., Rogers, A. E. E., Ball, J. A., Carter, J. C., and Cudaback, D. D. 1968, *Ap. J.* (*Letters*), **152**, L97.
Meulen, J. J. ter, and Dymanus, A. 1972, *Ap. J.* (*Letters*), **172**, L21.
Palmer, P., and Zuckerman, B. 1967, *Ap. J.*, **148**, 727.
———. 1970, *Ap. J.* (*Letters*), **161**, L199.
Rank, D. M., Townes, C. H., and Welch, W. J. 1971, *Science*, **174**, 1083.
Robinson, B. J., Goss, W. M., and Manchester, R. N. 1970, *Australian J. Phys.*, **23**, 363.
Rydbeck, O. E. H., Elldér, J., and Kollberg, E. 1969, *Ap. J.* (*Letters*), **156**, L141.
Rydbeck, O. E. H., Kollberg, E., and Elldér, J. 1970, *Ap. J.* (*Letters*), **161**, L25.
Schwartz, P. R., and Barrett, A. H. 1970, *Ap. J.* (*Letters*), **159**, L123.
Thacker, D. L., Wilson, W. J., and Barrett, A. H. 1970, *Ap. J.* (*Letters*), **161**, L191.
Turner, B. E., Palmer, P., and Zuckerman, B. 1970, *Ap. J.* (*Letters*), **160**, L125.
Weaver, H., Dieter, N. H., and Williams, D. R. W. 1968, *Ap. J. Suppl.*, **16**, 219.
Wilson, W. J., Barrett, A. H., and Moran, J. M. 1970, *Ap. J.*, **160**, 545.
Yen, J. L., Zuckerman, B., Palmer, P., and Penfield, H. 1969, *Ap. J.* (*Letters*), **156**, L27.
Zuckerman, B. 1971, in *Highlights of Astronomy*, ed. De Jager (Dordrecht: D. Reidel Publishing Co.).
Zuckerman, B., Ball, J. A., Dickinson, D. F., and Penfield, H. 1969, *Ap. Letters*, **3**, 97.
Zuckerman, B., and Palmer, P. 1970, *Ap. J.* (*Letters*), **159**, L197.